Theoretical Study on the Electronic Spectrum and the Origin of Remarkably Large Third-Order Nonlinear Optical Properties of Organoimide Derivatives of Hexamolybdates

Guochun Yang, Wei Guan, Likai Yan, and Zhongmin Su*

Institute of Functional Material Chemistry, Faculty of Chemistry, Northeast Normal University, Changchun 130024, People's Republic of China

Lin Xu and En-Bo Wang*

Institute of Polyoxometalate Chemistry, Faculty of Chemistry, Northeast Normal University, Changchun 130024, People's Republic of China

Received: May 8, 2006; In Final Form: September 6, 2006

Electronic spectrum of organoimide derivatives of hexamolybdates have first been calculated within the time-dependent density-functional theory in conjunction with Van Leeuwen−Baerends (LB94) exchange correlation potential, statistical average of orbital potentials (SAOP), and gradient-regulated connection potential (GRAC), respectively. The GRAC yields much better agreement with experiments for the excitation energies comparing with both LB94 and SAOP. The analysis of transition nature indicates that there is a significant difference between the diagonal and the orthogonal substituted derivatives. The static and dynamic third-order polarizabilities are calculated using time-dependent density-functional theory combined with the sum-over-states method. The results show that these derivatives possess remarkable large molecular third-order polarizabilities, especially for system 8 with -17882.6×10^{-36} esu. This value is about 250 times that for the C_{60} molecule. Adding the organoimide segment to the $[Mo_6O_{19}]^{2-}$ can substantially increase the γ value. This variation can be traced to the different electronic transition characteristics between the derivatives of $[Mo_6O_{19}]^{2-}$ and $[Mo_6O_{19}]^{2-}$. For our studied systems, increasing the conjugation length and diagonal substituted are efficient ways to enhance the third-order polarizability. Thus, the organoimide derivatives of hexamolybdates may comprise a new promising class of nonlinear optical materials from the standpoint of large γ values, small dispersion behavior, and high transparency.

1. Introduction

Polyoxometalates (POMs) are a rich class of inorganic cluster systems and exhibit remarkable chemical and physical properties, which have been applied to a variety of fields, such as medicine,[1] catalysis,[2] biology,[3] analytical chemistry,[4] and materials science.[5] The continued emergence for these applications will mainly depend on performance enhancement in such materials. POMs are electron acceptors, which in some cases can be reduced by one or more electrons, giving rise to mixed valency clusters. This enables the formation of organic−inorganic hybrid materials in which delocalized electrons coexist in both the organic networks and the inorganic clusters. Such materials not only combine the advantages of organic materials so as to realize the so-called value-adding properties, but also contribute to exploring the possible synergistic effects. Therefore, increasing attention is currently paid to make multifunctional hybrid materials by using covalently linked POMs and organic polymers. Judeinstein first reported the POM-polymer hybrid material in which a Keggin POM cluster was covalently linked to a polystyrene or polymethacrylate backbone through Si−O bonds.[6] Lalot and co-workers subsequently synthesized POM−polymer cross-linked networks.[7] Stein and co-workers prepared macroporous silica materials with POMs.[8] Especially, organoimide derivatives of Lindqvist-type POMs have expended quickly since Maatta and co-workers pioneered this field about 16 years ago.[9] Subsequently, a fairly large number of organoimide derivatives of POMs have been obtained, mainly based on the hexamolybdate ion $[Mo_6O_{19}]^{2-}$ as a building block.[10] Potential applications in molecular electronics and photonics of dumbbells and cis- or right-angled disubstituted derivatives have also been discussed by Peng and co-workers.[11]

Nonlinear optical processes are being increasingly exploited in a variety of optoelectronic and photonic applications. There exist three generic classes of NLO material: semiconductors, inorganic salts, and organic compounds. Each class possesses its own complement of favorable and unfavorable attributes for NLO application.[12] Semiconductors possess NLO effects originating from saturable absorption.[13] Their third-order NLO responses are among the largest known,[14] but NLO processes based on such resonant interactions may be relatively slow. Inorganic salts possess a large transparency range, are robust, are available as large single crystals, and suffer very low optical losses, but the purely electronic NLO effects are often accompanied by those arising from lattice distortions; response times are slow, and synchronization of the phase of the interacting optical fields is not easy to satisfy.[15] The organic materials are of major interest because of their relatively low cost, ease of fabrication and integration into devices, tailorability that allows one to fine-tune the chemical structure and properties for a given nonlinear optical process, high laser damage thresholds, low dielectric constants, fast nonlinear optical

* To whom correspondence should be addressed. Phone: +86-431-5099108. Fax: +86-431-5684009. E-mail: zmsu@nenu.edu.cn.

10.1021/jp062820p CCC: $33.50
Published on Web 10/20/2006

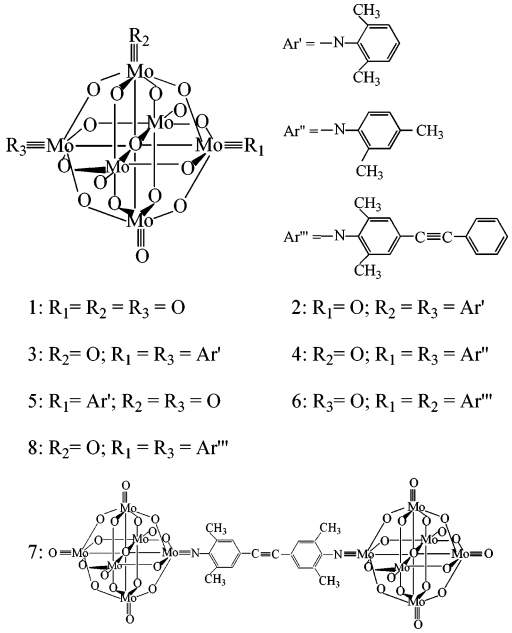

Figure 1. Calculation models.

response times, and off-resonance nonlinear optical susceptibilities comparable to or exceeding those of ferroelectric inorganic crystals.[16] Organic materials have several disadvantages: low energy transitions in the UV−vis region enhance the NLO efficiency but result in a tradeoff between nonlinear efficiency and optical transparency, they may have low thermal stability, and (in poled guest−host systems) they may undergo a facile relaxation to random orientation.[15] The limitations identified above spur investigations of new materials.

Among the many organic derivatives of POMs, organoidimide derivatives have been drawing increasing attention in that the strong d−π interaction between the organic delocalized π electrons and the cluster d electrons may result in fascinating synergistic effects.[17] The bonding character between arylimido and $[Mo_6O_{19}]^{2-}$ has been studied by our group.[18] The results show that the strong Mo≡N triple bond can be formed through the N → Mo σ-donation, N → Mo π-donation, and N ← Mo π-back-donation in the formation of the arylimido derivative. This strong interaction generates a strong electronic communication between arylimido and $[Mo_6O_{19}]^{2-}$. That is, the intramolecular electron transfer can occur and result in large nonlinear optical response. Our theoretical study has showed that those compounds have remarkable large second-order polarizability coefficients β.[19] Although, previous experiments[10a,h,11d,e] showed that bifunctionalized hexamolybdate derivatives preferred to form cis rather than trans structures, Wei and co-workers have recently synthesized trans structures (see Figure 1) and characterized UV−vis spectrum.[20] In view of the energy of the UV−vis spectrum, those structures satisfy high transparency in the visible-light area according to the research of Gompper et al.[21] These bifunctionalized hexamolybdate derivatives also have the strong Mo≡N triple bond character. It is expected that these derivatives offer some interesting new opportunities to the third-order nonlinear optical properties. Third-order nonlinear optical properties provide the basic means for controlling light with light (all optics), as in optical bistablility and phase conjugation. Moreover, the realization of all-optical switching, modulating, and computing devices is an important goal in modern optical technology, and NLO materials with large third-order polarizabilities are indispensable for such devices.

Density functional theory (DFT) has emerged as currently the most applied method for molecular computations due to its balance between accuracy and efficiency even for rather large systems. Improvements have been made by using the DFT investigation on POMs.[22] Our group has investigated the electronic properties, bonding character, stability, and NLO properties of POMs by DFT.[18,19,23] To our best knowledge, no theoretical effort has been put forth in an attempt to explain electronic spectrum and third-order NLO properties of bifunctionalized hexamolybdate derivatives. We used TDDFT method to calculate the UV−vis spectrum of organoimide hexamolybdate derivatives. The static and dynamic third-order NLO polarizabilities were then predicated by using TDDFT model combined with the sum-over-states (SOS) method in this paper.

2. Method and Computational Details

The DFT calculations were carried out using the ADF2003.01 suite of programs.[24] The zero-order regular approximation was adopted in all the calculations to account for the scalar relativistic effects.[25] The generalized-gradient approximation (GGA) was employed in the geometry optimizations by using the Beck[26] and Perdew[24] exchange-correlation (XC) functional. The basis functions were Slater-type sets. Triple-ζ plus polarization basis sets were used to describe the valence electrons of all the atoms, whereas for transition metal molybdenum atom, a frozen core composed of 1s to 3spd shells was described by means of single Slater functions. Moreover, the value of the numerical integration parameter used to determine the precision of numerical integrals was 5.5. Geometrical optimization of all systems under symmetry constraint was carried out, that is, O_h for system 1, C_{2v} for system 2, D_{2h} for system 3, and C_{2h} for system 4. Their structures are sketched in Figure 1. Systems 5−8 will be discussed in the following section.

The electronic spectrum was calculated based on the TDDFT. TDDFT has proved its efficiency in the evaluation of electronic spectra for a wide range of compounds. The XC effects in the ground state are represented with the local, state independent XC potential v_{xc} in the one-electron Kohn−Sham (KS) equations

$$\left[-\frac{1}{2}\nabla^2 + v_{ext}(r) + v_H(r) + v_{xc\sigma}(r)\right]\psi_{i\sigma}(r) = \epsilon_{i\sigma}\psi_{i\sigma}(r) \quad (1)$$

where v_{ext} is the external potential of the nuclei and v_H is the Hartree potential of electrostatic repulsion which, together with v_{xc}, define the KS orbital ψ_i and orbital energies ϵ_i. Because the exact form of v_{xc} is not known, various approximations are currently in use. Thus, accurate modeling of v_{xc} becomes an actual problem of TDDFT method. Even though the traditional local-density approximation (LDA) and GGA for v_{xc} have met with limited success, they consistently underestimate the zero-order excitation energy $\Delta\epsilon_{ia}$ for higher excitations due to the incorrect asymptotic behavior. Here, we have applied three different functionals for the zeroth-order potential: "Van Leeuwen−Baerends (LB94) XC potential" by Leeuwen and Baerends,[28] "statistical average of orbital potentials" (SAOP) by Gritsenko, Baerends et al.[29] and the "gradient-regulated connection potential" (GRAC).[30] These potentials have been developed specifically with the accuracy of excitation energies and response properties.[31]

The third-order polarizabilities were then calculated by using the SOS formula. The expression of third-order polarizabilities γ can be obtained by application of time-dependent perturbation theory to the interacting electromagnetic field and microscopic system, as described in the following:[32]

$$\gamma_{ijkl} = \frac{4\pi^2}{3\hbar^3} P(i, j, k, l; -\omega_\sigma, \omega_1, \omega_2, \omega_3) \times \sum_{m\neq g}\sum_{n\neq g}\sum_{p\neq g}\left[\frac{(\mu_i)_{gm}(\bar{\mu}_j)_{mn}(\bar{\mu}_k)_{np}(\mu_l)_{pg}}{(\omega_{mg} - \omega_\sigma - i\gamma_{mg})(\omega_{ng} - \omega_2 - i\gamma_{ng})(\omega_{pg} - \omega_3 - i\gamma_{pg})}\right] - \sum_{m\neq g}\sum_{n\neq g}\left[\frac{(\mu_i)_{gm}(\mu_j)_{mg}(\mu_k)_{gn}(\mu_l)_{ng}}{(\omega_{mg} - \omega_\sigma - i\gamma_{mg})(\omega_{ng} - \omega_2 - i\gamma_{ng})(\omega_{ng} - \omega_3 - i\gamma_{pg})}\right] \quad (2)$$

Here $(\mu_i)_{gm}$ is an electronic transition moment along the *i* axis of the Cartesian system, between the ground state and the excited state; $(\bar{\mu}_j)_{ng}$ is the dipole difference equal to $(\mu_j)_{mn} - (\mu_j)_{gg}$; ω_{mg} is the transition energy; ω_1, ω_2, and ω_3 are the frequencies of the perturbation radiation fields and $\omega_\sigma = \omega_1 + \omega_2 + \omega_3$ is the polarization response frequency; $P(i, j, k, l; -\omega_\sigma, \omega_1, \omega_2, \omega_3)$ indicates all permutations of ω_1, ω_2, ω_3, and ω_σ along with associated indices *i, j, k, l*; and γ_{mg} is the damping factor. When ω_σ or ω_1 approaches ω_{mg}, the eq 2 will diverge. According to the literature,[33] the damping factor is set to 0.1 eV in calculating the dynamic third-order polarizability. The transition energy, transition moments, and dipole moments can be obtained from the calculated results on the basis of the TD model of ADF. First, 100 excited states were calculated using the TD model of ADF for all compounds. Those physical values were then taken as input of the SOS formula to calculate the third-order polarizabilities. An amount equal to 100 excited states is enough according to the converge curves of SOS method (Supporting Information). Our group has used this method to investigate the NLO properties of a series of compounds.[34] In this paper, the symbols γ $(-3\omega; \omega, \omega, \omega)$, γ $(-2\omega; \omega, \omega, 0)$, and γ $(-\omega; \omega, -\omega, \omega)$ represent the third-order polarizability of third-harmonic generation (THG), electronic-field-induced second-harmonic generation (EFISHG), and degenerate four-wave mixing (DFWM), respectively.

3. Results and Discussion

3.1. Orbital Character. The diagrams for frontier molecular orbitals (FMO) of systems 1−4 are displayed in Figure 2. The highest occupied molecular orbital (HOMO) of system 1 formally delocalizes over the oxo ligands, and the lowest unoccupied molecular orbital (LUMO) is the symmetry-adapted d-metal orbital with some antibonding participation of O_p orbitals. Mo−O interaction has Mo_d-O_p character. For systems 2−4, one of the most striking features of these systems is the extensive π-electron delocalization over the organoimido segment and Mo atom with bonding to the N atom. The delocalized π bond coming from the carbon atoms of arylimido and the d−p π bond from the d_{xz} orbital on the molybdenum atom, which links the nitrogen atom and the p_x orbital on nitrogen, largely contribute to the HOMO, which implies a strong ground-state interaction between hexamolybdate and organoimido. The LUMO has a common character that the LUMO localizes over the Mo_d orbitals and O_p orbitals. This feature suggests that adding the organoimido segment to $[Mo_6O_{19}]^{2-}$ has no influence on the characters of LUMO comparing with $[Mo_6O_{19}]^{2-}$. In terms of FMO, as shown in Figure 2, systems 2−4 consist of a $[Mo_6O_{19}]^{2-}$ electron-withdrawing group centered between two electron-donating moieties. It indicates that those molecules possess donor−acceptor−donor (D−A−D) configurations (Figure 3).

To our studied systems, the efficiency of charge transfer mainly depends on degree of organic/inorganic interactions. The formation of the Mo≡N triple bond increases delocalization of the aromatic π electron and strong electronic interaction between the metal−oxygen cluster and the organoimido moiety.[18] This suggests that a high degree of intramolecular charge-transfer should be occurring, and a large third-order NLO response could be expected.

3.2. Electronic Spectrum. To find a better potential for calculating the excitation energy for our studied systems, three different xc potentials are used here. In Table 1, we list the calculated and experimental absorption λ_{max} values, oscillator strengths, and major contribution. From Table 1, It can be seen that the GRAC does lead to significantly better results than the SAOP functional and LB94 XC potential function. It can be explained by the following: the LB94 has the poor approximation in the region near the nucleus.[27c] Although both SAOP and GRAC correct the Kohn−Sham potential in particular in the outer "asymptotic" region and thus lead to much improved virtual orbitals and virtual orbital energies comparing with standard LDA or GGA potentials, GRAC can construct smooth asymptotically corrected potentials, which are genuine density functionals with an analytical representation.[30] This indicates that GRAC is the most suitable functional for our studied systems.

For system 1 (O_h symmetry), the transition energy is 315 nm, which is generated by promotion of one electron from HOMO−3 to LUMO+1. As a result of the HOMO−3 belonging to t_{1u} symmetry and the LUMO+1 belonging to t_{2g}, such electronic transition is dipole-allowed. This transition can be assigned to the charge-transfer transition from the bridging oxygen (O_b) to the terminal oxygen (O_t) and central oxygen (O_c), and there is charge transfer between the Mo atoms. For systems 2 (C_{2v} symmetry), HOMO−1 and LUMO+9 belong to a_2 and b_1, $a_2 \rightarrow b_1$ is dipole-allowed. This transition can be assigned to the charge-transfer transition from the organoimide segment to $[Mo_6O_{19}]^{2-}$. The transitions of system 3 and system 4 are also dipole-allowed. System 3 and system 4 have similar transition natures, which are the charge-transfer transitions from the O_t and Mo to the O_c and O_b. This implies that the substituted position of the methyl does not have any influence on the transition nature.

The computational results show that the energies of systems 2−4 are significantly red-shifted by comparison with system 1 and oscillator strengths are also strengthened considerably, indicating that a strong Mo−N bond is formed and the delocalization of the aromatic π electrons is increased. In other words, a strong electronic interaction between the metal−oxygen cluster and the organic segment occurs. There is little difference in the excitation energy resulting from substitutents of diagonal or orthogonal compared with that of systems 2 and 3. However, there is a distinct difference to the oscillator strengths. It indicates that system 3 has a larger transition probability than that of system 2. This can be associated with the different transition natures between the systems 2 and 3 (Figure 4).

3.3. Third-Order Polarizability. To find the influence on the third-order polarizability of the different substitutions and effective ways to get large third-order polarizability, the monosubstituted $[Mo_6O_{18}R]^{2-}$ (where R = 2,6-dimethylphenyl corresponds to system 5), disubstituted $[Mo_6O_{18}R_2]^{2-}$ (where R = 2,6-dimethyl-4-(2-p-tolylethynyl)benzenamine, the orthogonal derivative corresponds to system 6, and the diagonal derivative corresponds to system 8), and novel hybrid dumbbells[11c] (system 7) were studied here. Specific molecular structures are provided in Figure 1. The absorption spectrum values are 339, 381, 432, and 409 nm for systems 5, 6, 7, and 8, respectively. Although the systems 6, 7, and 8 have the increasing conjugation length, they can maintain the high transparency required, which

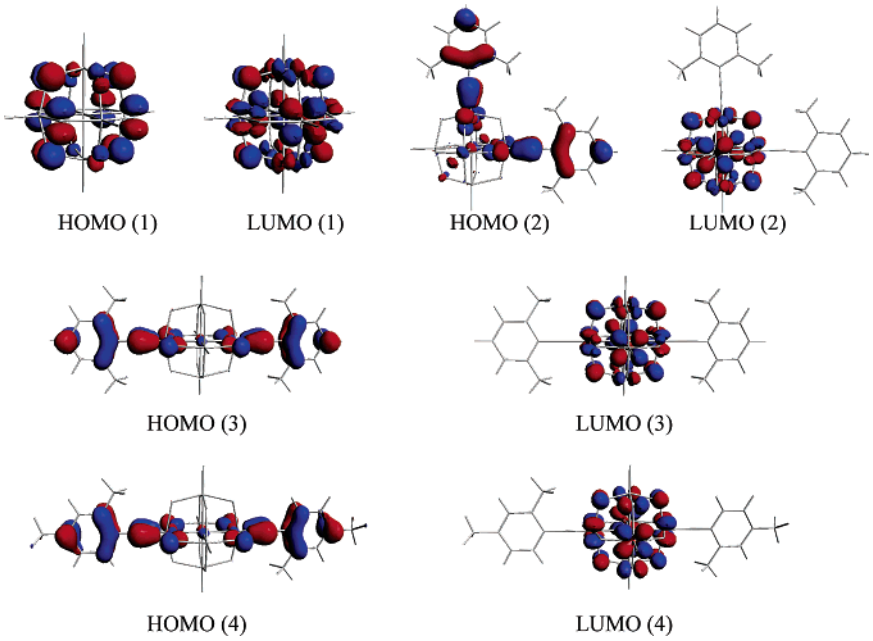

Figure 2. HOMO and LUMO of systems 1−4.

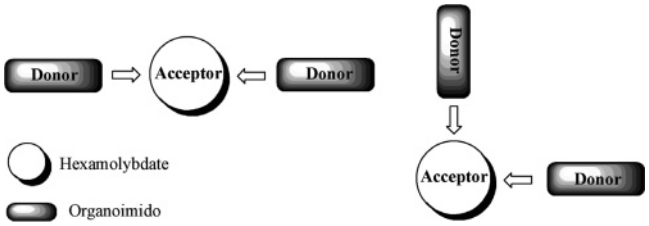

Figure 3. Sketch map of the D−A−D type POMs.

is worthy of remarks in considering practical application in the NLO field. An average γ is obtained from the expression $\gamma = 1/5(\gamma_{xxxx} + \gamma_{yyyy} + \gamma_{zzzz} + \gamma_{xxyy} + \gamma_{xxzz} + \gamma_{yyxx} + \gamma_{yyzz} + \gamma_{zzxx} + \gamma_{zzyy})$. The static third-order polarizability is termed the zero-frequency hyperpolarizability and is an estimate of the intrinsic molecular hyperpolarizability in the absence of resonance effect. These values are listed in Table 2. The calculated static third-order polarizability is several times larger than those of typical compounds with extensive π-electron conjugation. For example, the calculated γ value of system 4 is about 10 times larger than the average third-order polarizability of the C_{60} molecule[35] and 14 times larger than that measured for highly π-delocalized ruthenium(II) complexes.[36] Those indicate that the studied systems have excellent third-order nonlinear optical response.

The absolute γ value increases as follows: system 1 < 5 < 2 < 3 < 4 < 6 < 7 < 8. The results indicate that adding the organoimide segment to the $[Mo_6O_{19}]^{2-}$ leads to a substantial increment of the γ values. This can be associated to the different nature of the charge transition in these systems. To the SOS method, the third-order polarizability is governed by the product of the transition moments and the transition energy. From Table 1, the system 2 has larger oscillator strength than that of system 1. Oscillator strength is proportional to the transition energy and transition moment ($f = (8\pi^2 m_e/3e^2h)E_{ng}\mu_{ng}^2$). However, system 2 has a smaller transition energy compared to that of system 1. This implies that system 2 has the larger transition moment and leads to a larger charge transfer. Therefore, the larger charge transfer will come into being under the external electronic field. The diagonal substituted derivatives have larger γ values compared to those of orthogonal-substituted derivatives. It attributes to the diagonal substituted having a larger oscillator strength (for example, systems 3 and 4). But, there is little influence on the position of the methyl substitutent by comparing with systems 3 and 4. System 7 possesses acceptor−donor−acceptor (A−D−A) configurations (Supporting Information), which is different from systems 2, 3, 4, 6, and 8. Although system 7 (dumbbells structure) increases the γ value compared to that of systems 3 and 4, its γ value is smaller than that of system 8. Furthermore, the γ value of system 8 is about 27 times larger than that of system 3, which indicates that increasing the conjugation length can lead to substantial enhancement effects to the γ values. Moreover, all the systems have negative third-order polarizabilities, which are relatively uncommon. Such all-optical nonlinearities are self-defocusing, rather than self-focusing, eliminating the concern of the nonlinear optical auto-optical annihilation of a potential all-optical device. Additionally, negative γ have been instrumental in helping define the family of microscopic electronic mechanisms, which can contribute to γ.[37] Thus, these inorganic−organic hybrid materials may not only increase the third-order nonlinear optical response, but also offer greater scope for the creation of multifunctional nonlinear

TABLE 1: Calculated and Experimental Absorption λ_{max} (nm), Oscillators Strengths, Major Contribution, and Experimental Data for Systems 1−4

systems	LB94	SAOP	GRAC	exp	f^a	major contribution[a]
1	313	345	315	325[b]	0.0258	HOMO3(t_{1u}) →HardReturnLUMO+1(t_{2g})
2	332	348	358	354[b]	0.1976	HOMO1(a_2) →HardReturnLUMO+9(b_1)
3	340	365	360	358[b]	0.3417	HOMO5(b_u) →HardReturnLUMO+8(a_g)
4	345	373	370	361[c]	0.3353	HOMO5(b_{3u}) →HardReturnLUMO+10(b_{1g})

[a] Using the GRAC. [b] From ref 20a. [c] From ref 20b.

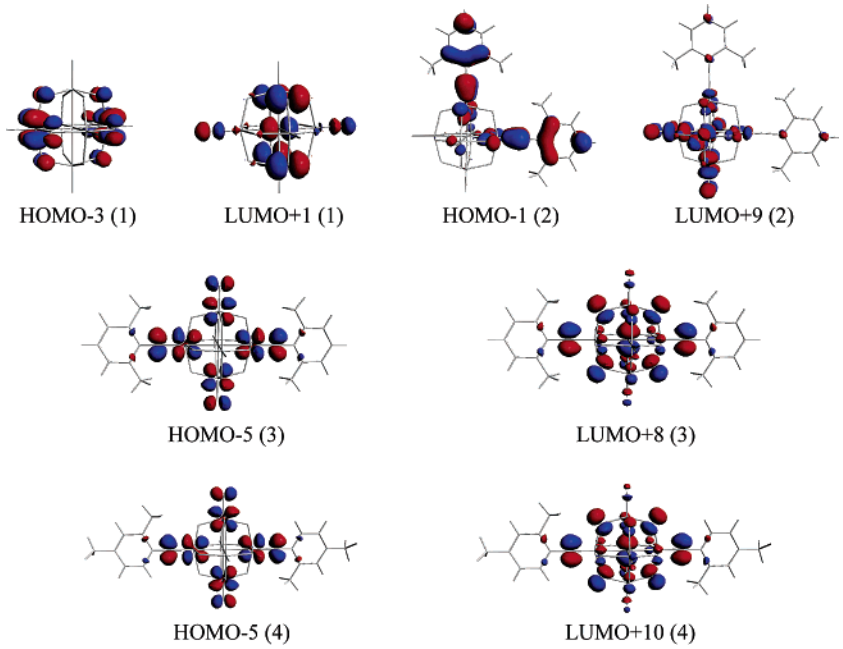

Figure 4. Molecular orbitals involved in the main energy transition.

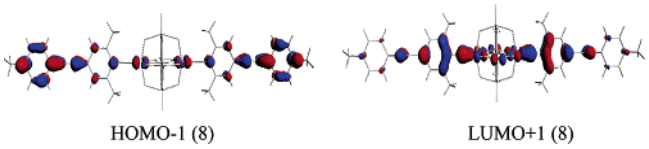

Figure 5. Molecular orbitals that make the main contribution to the NLO response of system 8.

TABLE 2: Static Third-Order Polarizability of the Studied Compound by GRACLB Functional (10^{-36} esu)

systems	γ
1	−38.2
2	−117.3
3	−659.7
4	−695.2
5	−57.5
6	−7636.1
7	−12 673.2
8	−17 882.6

optical materials when compared with that of purely organic or inorganic materials.

To understand the electronic origin of nonlinear optical responses for the system 8, the value of γ calculated from the 14th excited state is about 46.5% of the γ obtained from a summation of over 100 states, and the state 14 is a significant contribution to the third-order polarizability of the system 8. This state is generated by the promotion of one electron from the HOMO−1 to the LUMO+1 (see Figure 5). The orbital pattern suggests that this electronic transition should be attributed to charge transfer from the peripheral phenyl groups to the central core. That is, the charge transfer from the peripheral phenyl groups to the central core makes a substantial contribution to the third-order polarizability.

For system 8, the dynamic behaviors of the third-order polarizability of the considered nonlinear optical processes are plotted in Figure 6. In the THG process, there are ω, 2ω, and 3ω photon processes, and in the EFISH and DFWM processes, there are ω and 2ω enhancements. In the static case, which the input photon energy is zero, the value of all the three processes, THG, EFISHG, and DFWM, are the same. The curves appear as a small dispersion behavior at the low frequency (ω is below

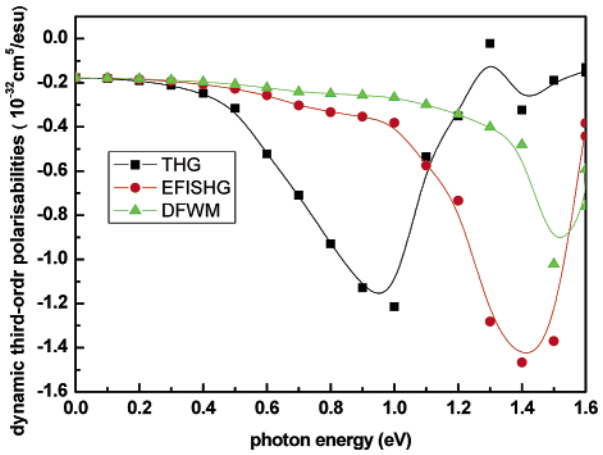

Figure 6. Dynamic third-order polarizabilities of the THG, EFISHG, and DFMW processes for system 8.

0.8 eV.) for all three processes. As excepted, the dynamic γ value occurs in the order γ ($-\omega$; ω, ω, $-\omega$) < γ (-2ω; ω, ω, 0) < γ (-3ω; ω, ω, ω) at below 0.8 eV. The low-lying electronic transition energy based on the result of the TDDFT calculation is about 3.03 eV. For incident frequency at about ω = 1.0 eV, the THG results suffer from resonant enhancement, because the triple of ω becomes close to the low-lying electronic transition energy. There is a resonant enhancement that appears at about ω = 1.4 and 1.5 eV for the EFISHG and DFWM, respectively. This can be attributed to 2ω, which is equal to the low-lying electronic transition energy. Accordingly, we can choose an input wavelength among the measuring techniques of the THG, EFISHG, and DFWM processes to obtain the nonresonant third-order polarizabilities from the known transition energy.

4. Conclusions

We have first investigated the electronic spectrum and the third-order nonlinear optical properties of the organoimide derivatives of hexamolybdates and the elucidated structure−property relationship from the micromechanism. The LB94, SAOP, and GRAC, which have been developed specifically with

the accuracy of excitation energies, were applied to these derivatives. The results show that the accurate electronic absorption spectrum of organoimide derivatives of hexamolybdates can be achieved using the GRAC. Adding the organoimide to $[Mo_6O_{19}]^{2-}$ can increase the transition probability compared to $[Mo_6O_{19}]^{2-}$. The transition nature of the diagonal-substituted derivatives is different from that of the orthogonal-substituted derivatives.

The static and dynamic third-order polarizabilities were then predicated by using the TDDFT model combined with the SOS method. The organoimide derivatives of hexamolybdates are found to possess remarkably larger static third-order polarizability compared with that of the typical organic compounds. Adding the organoimide segment to the $[Mo_6O_{19}]^{2-}$ can substantially increase γ values. This variation can be traced to the different electronic transition characteristics. Increasing the conjugation length can substantially enhance the γ values. The diagonal-substituted derivatives have larger γ values than orthogonal-substituted derivatives. This implies that the diagonal-substituted derivatives have a larger charge transfer than that of the orthogonal-substituted derivatives. A dynamic third-order NLO response shows that all the studied systems have small disperse behaviors. Thus, it can be concluded that these systems can be classified as a completely new kind of third-order nonlinear optical material from the viewpoint of the high transparency, small dispersion behavior and relatively large γ.

Acknowledgment. Authors acknowledge the financial support from the National Natural Science Foundation of China (Project No. 20373009 and 20573016) and the Specialized Research Fund for the Doctoral Program in Higher Education Institutions of the Ministry of Education of China (No. 20030183063) for financial support. Science Foundation for Young Teachers of Northeast Normal University (No. 20060307) is also greatly appreciated.

Supporting Information Available: Convergent behaviors of the third-order polarizabilities and the A−D−A configuration of system 7 and its frontier molecular orbitals. This material is available free of charge via the Internet at http://pubs.acs.org.

References and Notes

(1) (a) Rhule, J. T.; Hill, C. L.; Judd, D. A. *Chem. Rev.* **1998**, *98*, 327. (b) Hou, Y. Q.; Hill, C. L. *J. Am. Chem. Soc.* **1993**, *115*, 11823. (c) Hasenknopf, B. *Front. Biosci.* **2005**, *10*, 275.

(2) (a) Hill, C. L.; Prosser-McCartha, C. M. *Coord. Chem. Rev.* **1995**, *143*, 407. (b) Yin, C. X.; Sasaki, Y.; Finke, R. G. *Inorg. Chem.* **2005**, *44*, 8521. (c) Gong, Y.; Hu, C. W.; Liang, H. *Front. Biosci.* **2005**, *15*, 385.

(3) Muller, A. *J. Mol. Struct.* **1994**, *325*, 13.

(4) Proust, A. *Actual. Chim.* **2000**, *7*−*8*, 55.

(5) (a) Casan-Pastor, N.; Gomez-Romero, P. *Front. Biosci.* **2004**, *9*, 1759. (b) Rindel. M. S. *Afr. J. Sci.* **1916**, *11*, 362. (c) Chalkley, L. *J. Phys. Chem.* **1952**, *56*, 1084. (d) Chalkley, L. *J. Opt. Sci. Am.* **1954**, *44*, 699. (e) Chen, c.; Wu, B.; Jiang, A.; Wu. B.; You, G.; Li, R.; Lin, S. *J. Opt. Soc. Am.* **1989**, *B6*, 616. (g) Coronado, E.; Gomez-Garcia, C. J. *Chem. Rev.* **1998**, *98*, 273.

(6) Judeinstein, P. *Chem. Mater.* **1992**, *4*, 4.

(7) (a) Strong, J. B.; Yap, G. P. A.; Ostrander, R.; Liable-Sands, L. M.; Rheingold, A. L.; Thouvenot, R.; Gouzerh, P.; Maatta, E. A. *J. Am. Chem. Soc.* **2000**, *122*, 639. (b) Mayer, C. R.; Cabuil, V.; Lalot, T.; Thouvenot, R. *Angew. Chem.* **1999**, *111*, 3878. (c) Mayer, C. R.; Cabuil, V.; Lalot, T.; Thouvenot, R. *Angew. Chem., Int. Ed.* **1999**, *38*, 3672. (d) Mayer, C. R.; Thouvenot, R.; Lalot, T. *Chem. Mater.* **2000**, *12*, 57.

(8) (a) Schroden, R. C.; Blanford, C. F.; Melde, B. J.; Johnson, B. J. S.; Stein, A. *Chem. Mater.* **2001**, *13*, 1074. (b) Johnson, B. J. S.; Stein, A. *Inorg. Chem.* **2001**, *40*, 801.

(9) Du, Y.; Rheingold, A. L.; Maatta, E. A. *J. Am. Chem. Soc.* **1992**, *114*, 345.

(10) (a) Strong, J. B.; Ostrander, R.; Rheingold, A. L.; Maatta, E. A. *J. Am. Chem. Soc.* **1994**, *116*, 3601. (b) Stark, J. L.; Rheingold, A. L.; Maatta, E. A. *Chem. Commun.* **1995**, *11*, 1165. (c) Stark, J. L.; Young, V. G.; Maatta, E. A. *Angew. Chem., Int. Ed. Engl.* **1995**, *34*, 2547. (d) Strong, J. B.; Haggerty, B. S.; Rheingold, A. L.; Maatta, E. A. *Chem. Commun.* **1997**, *12*, 1137. (e) Proust, A.; Thouvenot, R.; Chaussade, M. F.; Robert, P. *Inorg. Chim. Acta* **1994**, *224*, 81. (f) Clegg, W.; Errington, R. J.; Fraser, K. A.; Lax, C.; Richards, D. G. In *Polyoxometalates: from Platonic Solid to Anti-retroviral Activity*; Pope, M. T., Muller, A., Eds.; Kluwer: Dordrecht, Germany, 1994; p 113. (g) Clegg, W.; Errington, R. J.; Fraser, K. A.; Holmes, S A.; Schafer, A. *Chem. Commun.* **1995**, *4*, 455. (h) Strong, J. B.; Yap, D. P. A.; Ostrander, R.; Liable-Sands, L. M.; Rheingold, A. L.; Thouvenot, R.; Gouzerh, P.; Maatta, E. A. *J. Am. Chem. Soc.* **2000**, *122*, 639. (i) Wei, Y.; Xu, B.; Barnes, C. L.; Peng, Z. *J. Am. Chem. Soc.* **2001**, *123*, 4083. (j) Peng, Z. M. *Angew. Chem., Int. Ed.* **2004**, *43*, 930. (k) Kang, J.; Nelson, J. A.; Lu, M.; Xie, B.; Peng, Z.; Powell, D. R. *Inorg. Chem.* **2004**, *43*, 6408. (l) Kang, J.; Xu, B.; Peng, Z.; Zhu, X.; Wei, Y.; Powell, D. R. *Angew. Chem., Int. Ed.* **2005**, *44*, 6902. (m) Xia, Y.; Wu, P.; Wei, Y.; Wang, Y.; Guo, H. *Cryst. Growth Des.* **2006**, *6*, 253.

(11) (a) Wei, Y.; Lu, M.; Cheung, C.; Barnes, C. L.; Peng, Z. *Inorg. Chem.* **2001**, *40*, 5489. (b) Xu, B.; Wei, Y.; Barnes, C. L.; Peng, Z. *Angew. Chem., Int. Ed.* **2001**, *40*, 2290. (c) Lu, M.; Wei, Y.; Xu, B.; Cheung, C.; Peng, Z.; Powell, D. *Angew. Chem., Int. Ed.* **2002**, *41*, 1566. (d) Xu, L.; Lu, M.; Xu, B.; Wei, Y.; Peng, Z.; Powell, D. *Angew. Chem., Int. Ed.* **2002**, *41*, 4129. (e) Lu, M.; Xie, B.; Kang, J.; Chen, F.-C.; Yang, Y.; Peng, Z. *Chem. Mater.* **2005**, *17*, 402. (f) Xu, B.; Lu, M.; Kang, J.; Wang, D.; Brown, J.; Peng, Z. *Chem. Mater.* **2005**, *17*, 2841. (g) Bar-Nahum, I.; Narasimhulu, K. V.; Weiner, L.; Neumann, R. *Inorg. Chem.* **2005**, *44*, 4900.

(12) Blau, W. *Phys. Technol.* **1987**, *18*, 250.

(13) Nie, W. *Adv. Mater.* **1993**, *5*, 520.

(14) Allen, S. *New Sci.* **1989**, 31.

(15) Powell, C. E.; Humphrey, M. G. *Coord. Chem. Rev.* **2004**, *248*, 725.

(16) Bredas, J. L.; Adant, C.; Tackx, P.; Persoons, A.; Persoons, B. M. *Chem. Rev.* **1994**, *94*, 243.

(17) Katsoulis, D. E. *Chem. Rev.* **1998**, *98*, 359.

(18) Yan, L. K.; Su, Z. M.; Guan, W.; Zhang, M.; Chen, G. H.; Xu, L.; Wang, E. B. *J. Phys. Chem. B* **2004**, *108*, 17337.

(19) Yan, L. K.; Yang, G. C.; Guan, W.; Su, Z. M.; Wang, R. S. *J. Phys. Chem. B* **2005**, *109*, 22332.

(20) (a) Xia, Y.; Wei, Y. G.; Wang, Y.; Guo, H. Y. *Inorg. Chem.* **2005**, *44*, 9823. (b) Qin, C.; Wang, X. L.; Xu, L.; Wei, Y. G. *Inorg. Chem. Commun.* **2005**, *8*, 751.

(21) Gompper, R.; Mair, H. J.; Polborn, K. *Synthesis* **1997**, *6*, 696.

(22) (a) Rohmer, M. M.; Bénard, M.; Blaudeau, J. P.; Maestre, J. M.; Poblet, J. M. *Coord. Chem. Rev.* **1998**, *98*, 1019. (b) Lopez, X.; Bo, C.; Poblet, J. M. *J. Am. Chem. Soc.* **2002**, *124*, 12574. (c) Bridgeman, A. J.; Cavigliasso, G. *Inorg. Chem.* **2002**, *41*, 3500.

(23) (a) Guan, W.; Yan, L. K.; Su, Z. M.; Liu, S. X.; Zhang, M.; Wang, X. H. *Inorg. Chem.* **2005**, *44*, 100. (b) Yan, L. K.; Su, Z. M.; Tan, K.; Zhang, M.; Qu, L. Y.; Wang, R. S. *Int. J. Quantum Chem.* **2005**, *105*, 32. (c) Guan, W.; Yan, L. K.; Su, Z. M.; Wang E. B.; Wang, X. H. *Int. J. Quantum Chem.* **2006**, *106*, 1860.

(24) (a) te Velde, G.; Bickelhaupt, F. M.; van Gisbergen, S. J. A.; Fonseca Guerra, C.; Baerends, E. J.; Snijders, J. G.; Ziegler, T. *J. Comput. Chem.* **2001**, *22*, 931. (b) Fonseca Guerra, C.; Snijders, J. G.; te Velde, G.; Baerends, E. J. *Theor. Chem. Acc.* **1998**, *99*, 391. (c) *ADF2002.03, SCM, Theoretical Chemistry*; Vrije Universiteit: Amsterdam, The Netherlands.

(25) van Lenthe, E.; Baerends, E. J.; Snijders, J. G. *J. Chem. Phys.* **1993**, *99*, 4597.

(26) Becke, A. D. *Phys. Rev. A* **1988**, *38*, 3098.

(27) Perdew, J. P. *Phys. Rev. B* **1986**, *33*, 8822.

(28) van Leeuwen, R.; Baerends, E. J. *Phys. Rev. A* **1994**, *49*, 2421.

(29) Schipper, P. R. T.; Gritsenko, O. V. S.; van Gisbergen, J. A.; Baerends, E. J. *J. Chem. Phys.* **2000**, *112*, 1344.

(30) Grüning, M.; Gritsenko, O. V.; Gisbergen, S. J. A.; Baerends, E. J. *J. Chem. Phys.* **2001**, *114*, 652.

(31) (a) Osinga, V. P.; van Gisbergen, S. J. A.; Snijders, J. G.; Baerends, E. J. *J. Chem. Phys.* **1997**, *106*, 5091. (b) van Gisbergen, S. J. A.; Snijders, J. G.; Baerends, E. J. *J. Chem. Phys.* **1998**, *109*, 10644. (c) van Gisbergen, S. J. A.; Rosa, A.; Ricciardi, G.; Baerends, E. J. *J. Chem. Phys.* **1999**, *111*, 2499. (d) Autschbach, J.; Ziegler, T.; van Gisbergen, S. J. A.; Baerends, E. J. *J. Chem. Phys.* **2002**, *116*, 6930. (e) Grüning, M.; Gritsenko, O. V.; van Gisbergen, S. J. A.; Baerends, E. J. *J. Chem. Phys.* **2002**, *116*, 9591. (f) Ricciardi, G.; Rosa, A.; Baerends, E. J. *J. Phys. Chem. A* **2001**, *105*, 5242. (g) Rosa, A.; Ricciardi, G.; Baerends, E. J.; van Gisbergen, S. J. A. *J. Phys. Chem. A* **2001**, *105*, 3311.

(32) Orr, B. J.; Ward, J. F. *Mol. Phys.* **1971**, *20*, 513.

(33) (a) Albota, M.; Beljonne, D.; Bredas, J. L.; Ehrlich, J. E.; Fu, J. Y.; Heikal, A. A.; Hess, S. E.; Kogej, T.; Levin, M. L.; Marder, S. R.; McCord-Maughon, D.; Perry, J. W.; Rockel, H.; Rumi, M.; Subramaniam, C.; Webb, W. W.; Wu, X. L.; Xu, C. *Science* **1998**, *281*, 1653. (b) Rumi, M.; Ehrlich, J. E.; Heikal, A. A.; Perry, J. W.; Barlow, S.; Hu, Z.; Maughon, D.; Parker, T. C.; Rockel, H.; Thayumanavan, S.; Marder, S. R.; Beljonne, D.; Bredas, J.-L. *J. Am. Chem. Soc.* **2000**, *122*, 9500. (c) Masunov, A.; Tretiak, S. *J. Phys. Chem. B* **2004**, *108*, 899.

(34) (a) Yang, G. C.; Su, Z. M.; Qin, C. C.; Zhao, Y. H. *J. Chem. Phys.* **2005**, *123*, 134302. (b) Yang, G. C.; Qin, C. C.; Su, Z. M.; Shi, D. *THEOCHEM* **2005**, *726*, 61. (c) Yang, G. C.; Shi, D.; Su, Z. M.; Qin, C. C. *Acta Chim. Sin.* **2005**, *63*, 184. (d) Qin, C. C.; Yang, G. C.; Su, Z. M.; Zhu, Y. L.; Zhou, Z. Y. *Chem. J. Chin. Univ.* **2005**, *26*, 290. (e) Yang, G. C.; Su, Z. M.; Qin, C. C. *J. Phys. Chem. A* **2006**, *110*, 4817. (f) Yang, G. C.; Liao Y.; Su, Z. M.; Zhang, H. Y.; Wang, Y. *J. Phys. Chem. A* **2006**, *110*, 8758.

(35) Wang, Y.; Cheng, L. T. *J. Phys. Chem.* **1992**, *96*, 1530.

(36) Hurst, S. K.; Cifuentes, M. P.; Morrall, J. P. L.; Lucas, N. T.; Whittall, I. R.; Humphrey, M. G.; Asselberghs, I.; Persoons, A.; Samoc, M.; Luther-Davies, B.; Willis, A. C. *Organometallics* **2001**, *20*, 4664.

(37) (a) Dirk, C. W.; Cheng, L.-T.; Kuzyk, M. G. *Int. J. Quantum Chem.* **1992**, *43*, 27. (b) Dirk, C. W.; Cheng, L.-T.; Kuzyk, M. G. *Mater. Res. Soc. Symp. Proc.* **1992**, *247*, 73. (c) Gorman, C. B.; Marder, S. R. *Proc. Natl. Acad. Sci. U.S.A.* **1993**, *90*, 11297.